JOURNAL OF AIRCRAFT
Vol. 41, No. 5, September–October 2004

Aerodynamic Wing Design of NEXST-2 Using Unstructured-Mesh and Supersonic Inverse Problem

Takeshi Fujita,* Kisa Matsushima,† and Kazuhiro Nakahashi‡
Tohoku University, Sendai 980-8579, Japan

An efficient aerodynamic design system is developed and applied to design natural laminar flow wings of the experimental supersonic airplanes of the National Aerospace Laboratory (NAL) in Japan. In the design system developed, an inverse problem solver using integral equations is employed in the design phase, whereas unstructured-mesh computational-fluid-dynamics technology is used in the analysis phase so as to treat full configurations of airplanes efficiently. Interfaces among the design phase, the analysis phase, and the three-dimensional modeling phase are also developed. The rationale for the interface software implementation is described from the viewpoint of a practical aircraft design. The newly developed method has advantages of efficiency and wide applicability to complicated configurations of airplanes. Its capability is demonstrated for the wing design of the NAL NEXST-2 coupled with flow analysis of the full configuration.

Nomenclature

C_D	=	drag coefficient
C_L	=	lift coefficient
Cp	=	pressure coefficient
Cp_+	=	Cp at upper surface of wing
Cp_-	=	Cp at lower surface of wing
Cp^C	=	current Cp
Cp^T	=	target Cp
f	=	z coordinate of wing surface
M_∞	=	freestream Mach number
T/C	=	thickness to chord ratio
x_{LE}	=	x coordinate of leading edge
x_{TE}	=	x coordinate of trailing edge
$(x, y, z), (\xi, \eta, \zeta)$	=	Cartesian coordinate systems
ΔCp	=	$Cp^T - Cp^C$
Δf	=	geometrical correction value
ΔT	=	thickness correction value
$\Delta\phi$	=	perturbation velocity potential

Introduction

CURRENTLY, a next-generation supersonic transport is under development by the National Aerospace Laboratory (NAL) in Japan,[1] in collaboration with industries and universities, one of which is the Tohoku University. As part of this project, several airplane models are being developed for flight testing. The scale of those models is $\frac{1}{10}$ of real commercial passenger airplanes. In the first stage of this project, called NEXST-1 (see Fig. 1), an unpowered supersonic experimental airplane was developed, which will be launched for flight tests at the Woomera prohibited area in Australia in early 2004. In the second stage called NEXST-2, an experimental airplane equipped with an existing jet propulsion system, YJ-69, is under development, and the aerodynamic design of the first configuration has been finished as a prototype model (see Fig. 2). We, the Tohoku University team, are expected to design an improved configuration that has excellent aerodynamic characteristics.

With regard to wing design, an important aim of the NAL project is to reduce the drag by applying the concept of natural laminar flow (NLF) on the upper surface of the inner part and elliptical load distribution along the spanwise direction. Another aim is to establish a computational-fluid-dynamics (CFD)-oriented design system, a relatively new technology. This is one of the first projects to utilize CFD as a main tool for conceptual and initial aerodynamic design. With the design goal of the NLF concept, airfoil geometry must be precisely designed at each span station so as to realize a special form of pressure distribution on the wing surface under cruising conditions.[2] For this purpose, a new inverse design method, which can determine the airfoil geometry at each span station using specified pressure distribution as a boundary condition, has been formulated and developed.[3–5] The design method was derived from Takanashi's method. However, the present method is not just the application of Takanashi's because the present one is for supersonic, whereas Takanashi's is for transonic ($M_\infty < 1$) flows.[6] The fundamental equations of the corresponding inverse problem are different from each other. The wing design has been achieved using a combination of the supersonic inverse problem solver and conventional structured-mesh CFD for the NEXST-1. The NEXST-1 does not have a propulsion system, and thus, as shown in Fig. 1, the configuration is relatively simple.

In general, most design algorithms require several hundred flow simulations during the design process, whereas for the inverse design system it is known that the required number of flow simulations is less than 20, which is a very small number as compared with other design methods.[7] Even with this small number of simulations, it took several months to complete one design by the conventional CFD system because of the time-consuming process of mesh generation for the new complicated configuration.

One example of a complicated configuration is the NEXST-2 model, which has a fairly large propulsion system. Therefore, the interaction between the wing and the propulsion system must be taken into account (see Fig. 3). High-quality mesh is required for accurate simulation. However, the geometrical complexity makes it extremely difficult to use a structured mesh because of the painfully time-consuming mesh generation. To overcome this problem, unstructured-mesh CFD is utilized in this study. The preprocess of unstructured mesh generation has been already systematized (see Fig. 4). In addition, the computational time of the flow solver is drastically reduced by the lower-upper symmetric Gauss–Seidel (LU-SGS) implicit method and parallelization using the message-passing-interface (MPI) library. This aerodynamic

Received 30 June 2003; revision received 28 September 2003; accepted for publication 29 September 2003.

*Ph.D. Candidate, Department of Aeronautics and Space Engineering, Aramaki-Aza-Aoba 01, Aoba-ku. Member AIAA.
†Associate Professor, Department of Aeronautics and Space Engineering, Aramaki-Aza-Aoba 01, Aoba-ku. Senior Member AIAA.
‡Professor, Department of Aeronautics and Space Engineering, Aramaki-Aza-Aoba 01, Aoba-ku. Associate Fellow AIAA.

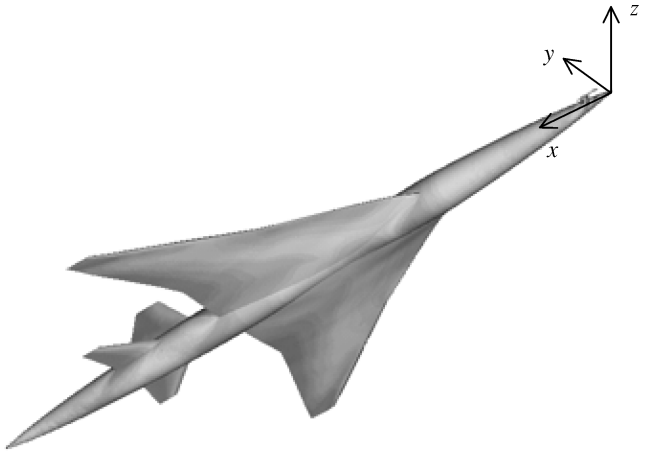

Fig. 1 Pressure distribution of NEXST-1 at $M_\infty = 2.0$ and $\alpha = 0.0$ deg.

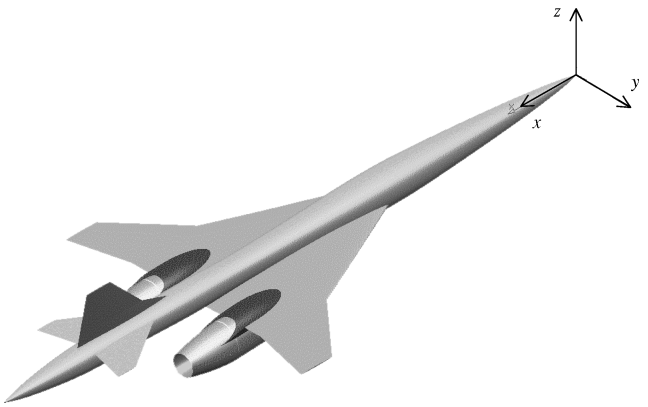

Fig. 2 First configuration of NAL NEXST-2.

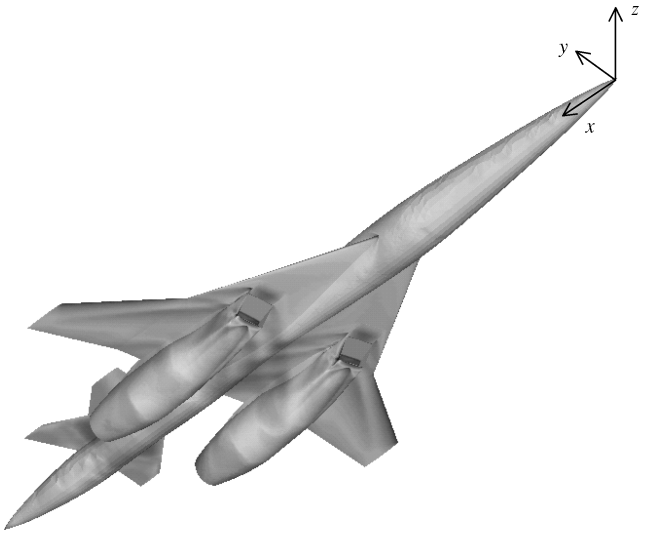

Fig. 3 Pressure distribution of NEXST-2 at $M_\infty = 1.7$ and $\alpha = 0.0$ deg.

evaluation system is able to realize "one-day CFD," which takes only one day per flow simulation.

As well as the necessity of efficient evaluation of aerodynamic performance for a complex configuration, it is also necessary to effectively combine the evaluation system with the inverse problem solver. Such interfacing is important for actual airplane design. The inconsistent usage of boundary conditions for the inverse solver and the CFD simulation causes unnecessary time-consuming effort, such as changes of setting angles, redefinition of new geometry,

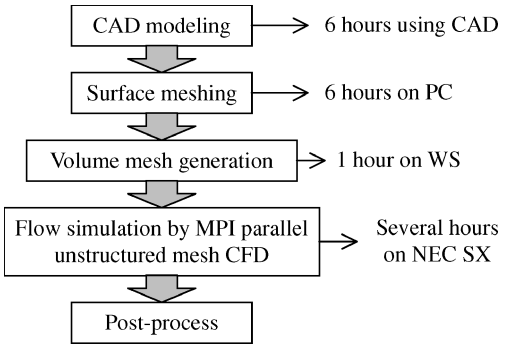

Fig. 4 CFD process.

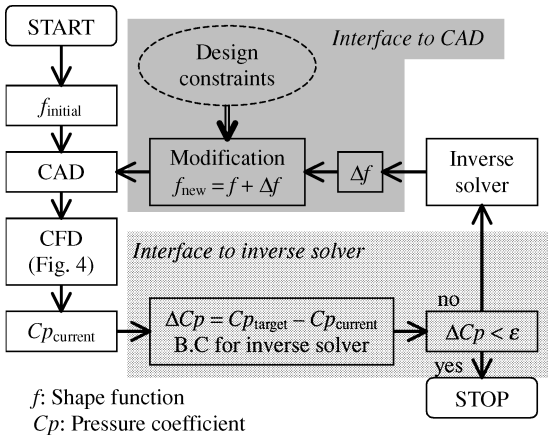

Fig. 5 Design procedure.

and so on. In this paper, a short turnaround inverse design system that can execute one cycle of inverse design loop in less than one day is described, where the inverse problem solver is effectively coupled with the unstructured-mesh CFD system. The capability of the system is demonstrated by applying it to the wing design of the NEXST-2 model.

Inverse Design and the Interface with CAD and CFD

The present design procedure for wings is an iterative method. Figure 5 illustrates the procedure. The method determines the geometry of the wing section, which realizes a specified target pressure distribution at all span stations of a wing. First, a baseline shape must be arbitrarily assigned. Then the flowfield around the wing is analyzed by flow simulation to obtain the Cp^C distribution on the wing surface. Next, the inverse problem is solved to obtain the Δf corresponding to the ΔCp. The new wing is defined by modifying the baseline shape using Δf. Now, the current shape is updated. The next step is to go back to the flowfield analysis, which is conducted to determine whether the current shape realizes target pressure distribution or not. If the difference between the target and the current pressure distributions is negligible, the design is completed; otherwise, the next step is to once again solve the inverse problem and iterate the design loop until the pressure difference becomes negligible. This iterative procedure of reducing the residual is widely used in numerical aerodynamic designs.

The inverse problem is formulated as two integral equations. This formulation is similar to the singularity source method based on small perturbation and the thin wing theory.[8] Thus, we consider an isolated wing for the inverse problem. The integral equations are solved using piecewise function approximation, in which the wing surface is descretized into small rectangular panels. With the descretization, an integral becomes the summation of each panel's value. An algebraic linear equation system instead of integral equations is solved. In case of the half-span model divided into 82

(spanwise) × 50 (chordwise) panels, the inverse solver can be finished in about 20 min using Intel Pentium 4 with a speed of 2.0 GHz. The following two subsections describe important modules to make the design procedure more practical for realistic designs.

Interface Between Flow Simulation and Inverse Design

The wing near the symmetry plane is overlapped by the fuselage, but the wing should continue to the fuselage center to solve the inverse problem. The wing-section airfoil and *Cp* distribution at the part covered by the fuselage are virtually generated by linearly extrapolating the 15% semispan airfoil, as shown in Fig. 6. For the extrapolation, quadratic extrapolation of the leading/trailing edge is performed inside a 3% semispan to connect the leading-edge curve smoothly to the opposite side of a half-wing span at the symmetry plane. This implies the removal of the apex singularity for discrete numerical computations.

Interface Between Inverse Design and CAD

The inverse problem solver in this study is formulated from the supersonic small perturbation theory,[5] and thus perturbation of the freestream direction, which is chordwise, is mostly considered. Accordingly, the solver handles the smoothness in the chordwise direction, not in the spanwise direction. Therefore, the geometry determined by the inverse problem sometimes oscillates in the spanwise direction. This causes a harmful effect on the following process of the design loop, and so the designed geometry is smoothed using least-squares approximation by a fifth-degree polynomial function, as shown in Fig. 7. Corresponding with the smoothing operation, in the CAD process with CATIA, spline curve is defined as an ordered set of joined arcs mathematically defined by single parameter fifth-degree polynomial functions.[9]

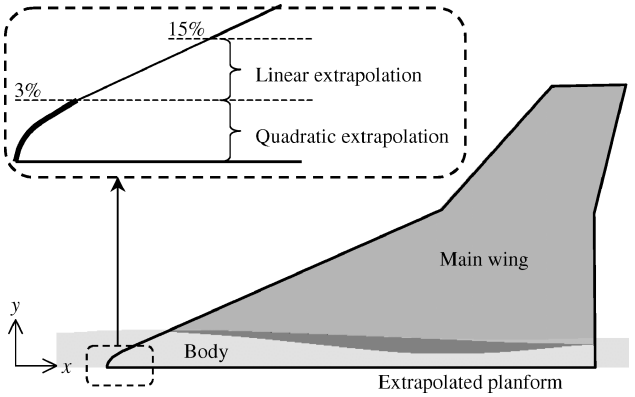

Fig. 6 Extrapolated wing planform.

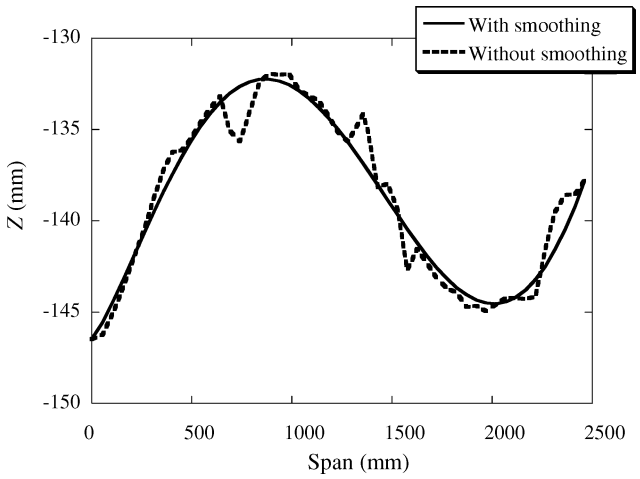

Fig. 7 Comparison of trailing-edge line in spanwise direction with/without smoothing.

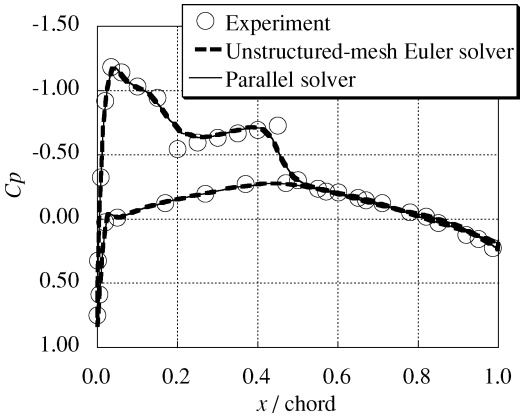

Fig. 8 *Cp* distributions for ONERA M6 at 65% semispan station.

CFD Evaluation System

The CFD preprocess of unstructured mesh has been already systematized (see Fig. 4). A configuration is defined using one of the most widely used commercial CAD software programs, CATIA. Several modification techniques, devised by one of the authors, are applied, and surface geometry data are obtained by a stereolithography file.[10] Then Edge Editor, a surface meshing software developed at Tohoku University,[11] is used to generate the surface mesh with the advancing front method. Finally, the volume mesh is automatically generated using Delaunay tetrahedral meshing.[12]

The Euler equations are solved by a solution algorithm based on a finite volume cell-vertex scheme for arbitrary shaped cells.[13] The control volume is dual cells with no overlap constructed around each node. To enhance the accuracy, a linear reconstruction of the primitive variables inside the control volume is applied with Venkatakrishnan's limiter.[14] The flux is computed using the HLLEW approximate Riemann solver.[15] The computational efficiency is improved by the Lu-SGS implicit method with a reordering algorithm for an unstructured mesh.[13] This implicit time-integration method does not require extra storage, and its performance is similar to that of structured mesh schemes. Further reduction of the computational time is introduced by parallelizing the unstructured-mesh CFD solver using the MPI library.[16,17] First, an unstructured volume mesh is divided by the mesh partitioner based on METIS, which was developed at the University of Minnesota.[18,*] Then the partitioned subdomains are distributed to each processor of a cluster of computers for the parallel execution. The neighboring subdomains are overlapped by one mesh cell. The physical quantity, gradient, and numerical flux at overlapping nodes are sent from "sending vertex" to corresponding "receiving vertices" in other subdomains. The *Cp* distribution for ONERA M6 at the 65% semispan station using the parallel solver is compared with the original Euler solver and the experiment data in Fig. 8. This figure indicates that the verification of this parallel solver is sufficiently good. Acceleration results for a large-sized Navier–Stokes (NS) computation on the NEC SX-4 vector computer of the Super-Computing System Information Synergy Center at Tohoku University are shown in Fig. 9. The hybrid mesh contains 2,180,582 nodes; 3,839,284 tetrahedrons; and 2,943,184 prisms; and this NS computation requires a memory of 4 GB. This parallel solver achieves extremely good scalability.

Inverse Design for NAL NEXST-2 Wing

The main wing of the NAL NEXST-2 model is designed using the inverse design system. The inner part of the wing is designed to be an NLF wing, and the outer part is designed to satisfy elliptical load distribution. This NLF concept and load requirement are embodied by a Cp^T distribution. Flat-roof-type *Cp* distribution on the upper surface keeps the laminar boundary layer as long as possible and reduces the friction drag. Furthermore, elliptical load distribution

*Data available online at http://www-users.cs.umn.edu/~karypis/.

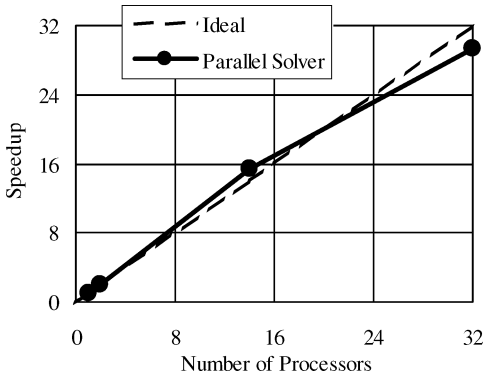

Fig. 9 Speedup for large-sized NS computation (4 GB) on NEC SX-4.

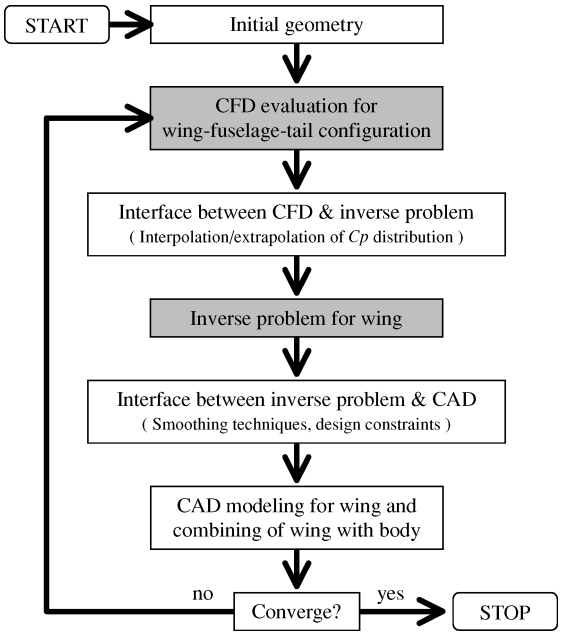

Fig. 10 Inverse design procedure for wing design of NEXST-2 model.

minimizes the induced drag. Along with the Euler equations solved for the wing-body-tail configuration, the inverse problem solver determines geometry for the wing to achieve the Cp^T.

Figure 10 shows this inverse design procedure for the NEXST-2 model wing. Because of the time limits of the project, we adopted a simple but presumably fast strategy, namely, a pseudonacelle approach. Thus, we assumed that the interaction effect between a wing and a nacelle is linear, as shown in Fig. 11. This is justified by Fig. 12, which shows a comparison of C_L with and without a nacelle. This figure also indicates that the effect of the nacelle interaction on C_L is constant at 0.06. Then, based on the pseudonacelle approach, a wing is designed with a constraint to maintain C_L at C_L^*, which is equivalent to $C_L - 0.06$. The target pressure distribution for the inverse problem solver is prescribed to satisfy the C_L condition. In other words, the preliminary design at the first stage is done without considering the nonlinear effect of the nacelle. To realize the design, the design system has been customized by introducing the following functions and strategies.

Evaluation of the Quality of Current Design

The quality of a design evaluated by the residual is defined as

$$\text{Residual} = \sqrt{\sum_{i=1}^{N} \left(Cp_i^T - Cp_i^C\right)^2} \Big/ N$$

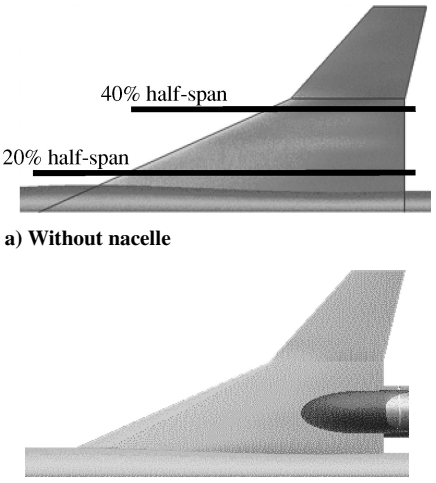

a) Without nacelle

b) With nacelle

Fig. 11 Upper-surface geometry of main wing with/without nacelle.

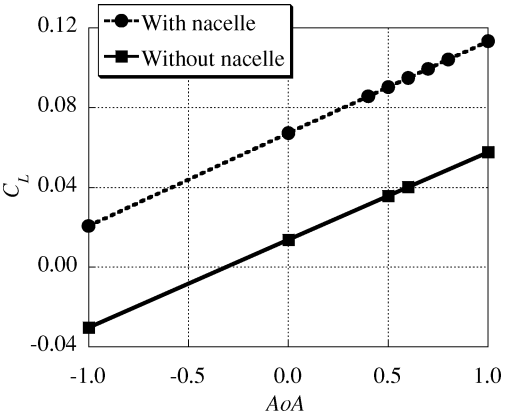

Fig. 12 Comparison of C_L with/without nacelle.

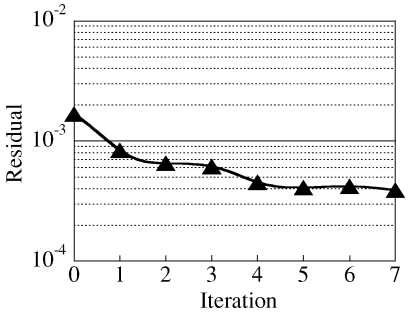

Fig. 13 Convergence history.

where Cp_i^T and Cp_i^C indicate target and current pressure coefficient distributions at each node point and N is the number of nodes on the wing surface. The convergence history of the process of NEXST-2 wing inverse design is shown in Fig. 13. The convergence rate was quantified with the residual. This residual function can be used as a standard indicator for the quality of the inverse design and a criterion to judge the design convergence.

Strategy to Satisfy Thickness Constraint

Because this is a design for a real flight model, many constraints must be satisfied. Thickness is one of the most important design constraints. On this NEXST-2 project, the wing thickness is constrained by the lowest limit for maximum T/C (max T/C) at each span to maintain structural strength. This is because the airplane has to support a propulsion system, which is quite large in comparison with the body. For this NEXST-2 design, the thickness constraint was

given first priority. Sometimes, thickness constraint is not consistent with the target pressure distribution. In such a case, the achievement of the Cp^T at the rear part of the wing, which is after 70% chord length, could be lost. The Cp^T does not have to be achieved after 70% chord. In fact, because the nacelle protrudes on the upper surface at the rear part of the wing, as shown in Fig. 11, it would disturb the Cp distribution after 70% chord length.

To keep the max T/C more than or equal to the value of the baseline at each span station, we propose the following measure for this NEXST-2 design, a combination of two items. One concerns the definition of a target pressure, and the other is the procedure to satisfy the closure condition of the trailing edge of a wing-section airfoil. According to the two-dimensional supersonic linear theory, the thickness change is proportional to the difference of the averaged Cp between the Cp^T and the Cp^C distributions. The averaged Cp is given by $\frac{1}{2}(Cp_+ + Cp_-)$. If the averaged Cp^T is higher than that of the current one, the thickness change is positive. Thus, the thickness can be controlled if the target pressure distribution is well defined. This would be true if we considered the direct solution of the mathematical inverse problem. In this design system, however, we must process the direct solution of the inverse problem to satisfy the condition that the airfoil has to have a closed trailing edge.[19] Thus, resulting wing-section airfoils do not always satisfy thickness requirements (Fig. 14a, target 1) with some given target pressure distributions. Without the procedure for closure condition, target 1 yields the same geometry for the airfoil. Thus, the Cp^T distribution is changed to target 2. Without the trailing-edge closure condition, target 2 results in a thicker airfoil geometry with an open trailing edge. However, the wing-section airfoils do not become thicker, even if the given target pressure has a higher average Cp, when the designer uses the present inverse problem solver (Fig. 14a, target 2 with closure condition). This is because the closure condition disturbs the thickness change. In such a case, the procedure for modifying the geometry correction to close the airfoil in the inverse problem solver should be changed.

The design of the NEXST-2 model is conducted in the following manner, when the thickness constraint is not satisfied. First, we determine the appropriate average Cp value level for the target pressure distribution and update it. Then, using the updated target pressure, we solve the inverse problem with the process for closure condition. The procedure utilized to compute the modified geometrical correction value is as follows:

$$\Delta T^{(\mathrm{mod})}(x, y) = \Delta T^{(direct)}(x, y) - \frac{\int_{x_{\mathrm{LE}}}^{x_{\mathrm{TE}}} \Delta T^{(direct)}(\xi, y)\, \mathrm{d}\xi}{\int_{x_{\mathrm{LE}}}^{x_{\mathrm{TE}}} \mathrm{d}\xi}$$

$$x_{\mathrm{LE}} \le x \le x_{\mathrm{TE}} \quad (1)$$

When the preceding results in undesired thin wing sections, the procedure is changed to

$$\Delta T^{(\mathrm{mod})}(x, y) = \begin{cases} \Delta T^{(direct)}(x, y) & x_{\mathrm{LE}} \le x \le x_0 \\ \Delta T^{(direct)}(x, y) - \dfrac{\int_{x_{\mathrm{LE}}}^{x_{\mathrm{TE}}} \Delta T^{(direct)}(\xi, y)\, \mathrm{d}\xi}{\int_{x_0}^{x_{\mathrm{TE}}} \mathrm{d}\xi} & x_0 < x \le x_{\mathrm{LE}} \end{cases} \quad (2)$$

We found the most appropriate x_0 location by solving the inverse problem with varying x_0 values for satisfying the closure condition (Fig. 14b). Equation (2) means that the geometry correction of the direct solution is not modified at locations before the x_0 chord position (Fig. 14b) closure condition after 70%). For this design problem, x_0 was set to 70% chord length.

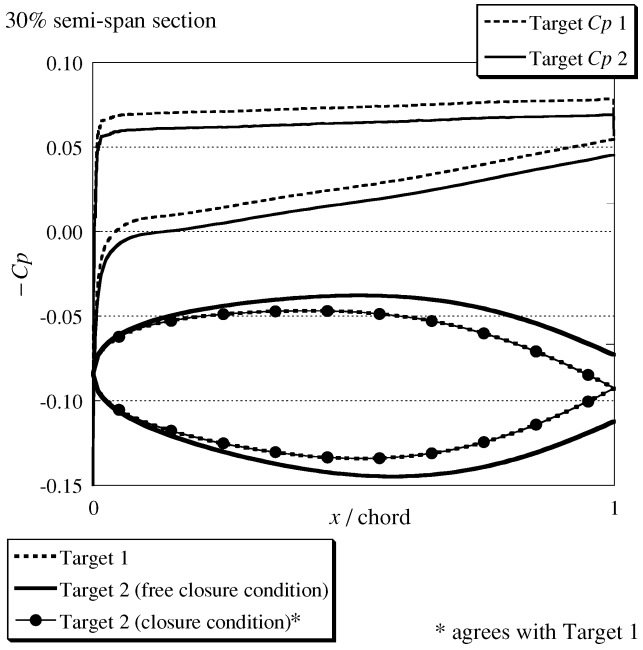

a) Comparison of two target C_p

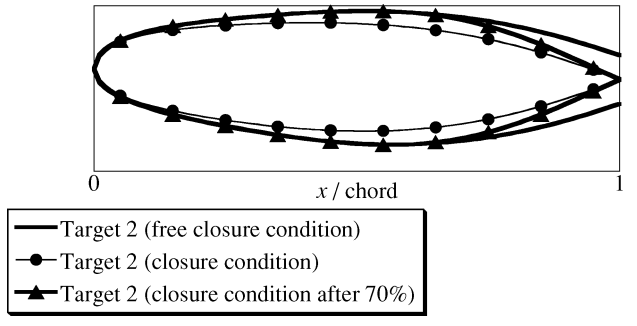

b) Closer condition

Fig. 14 Closer condition of trailing edge.

Visualization for Smoothness of Designed Geometry

The inverse problem based on the iterative residual-correction method used in this study does not consider the spanwise velocity component of perturbation velocity potential ($\Delta\phi_y$). The solution sometimes oscillates in the spanwise direction. Although a smoothing algorithm using the least-squares approximation by a fifth-degree polynomial function is applied to settling the oscillation, wing geometry in the spanwise direction sometimes presents structural and especially manufacturing difficulties. To examine this difficulty, z coordinates at constant x/chord are visualized as Fig. 15. Figure 15 shows surface z coordinates at the leading edge, at 25, 50, and 75% chord length positions and at the trailing edge in the spanwise direction of the inverse designed geometry. This visualization

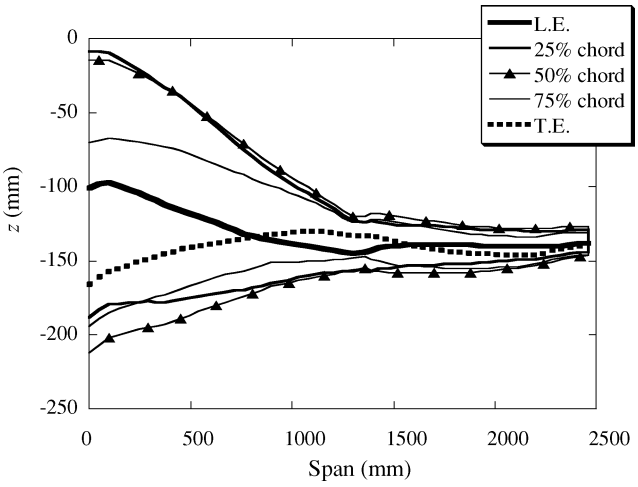

Fig. 15 Z coordinates at constant x/chord of designed geometry after three iterations.

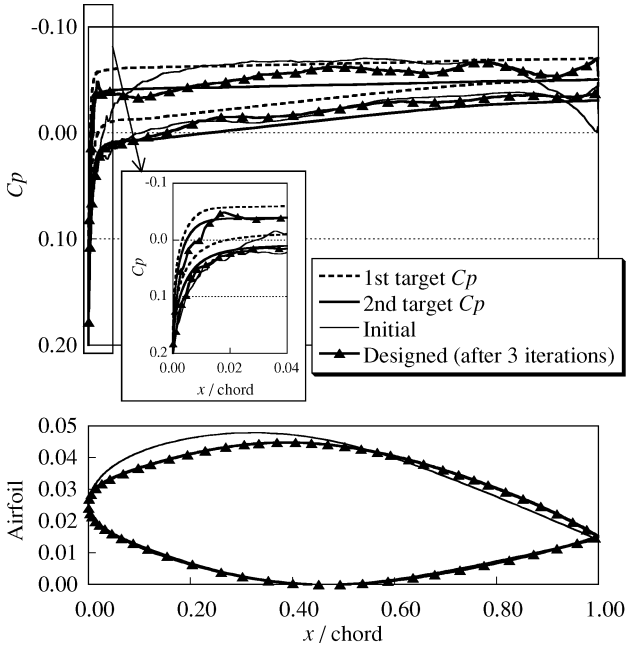

Fig. 16 Comparison of two targets and of initial and resulting airfoil after three design iterations at 20% semispan.

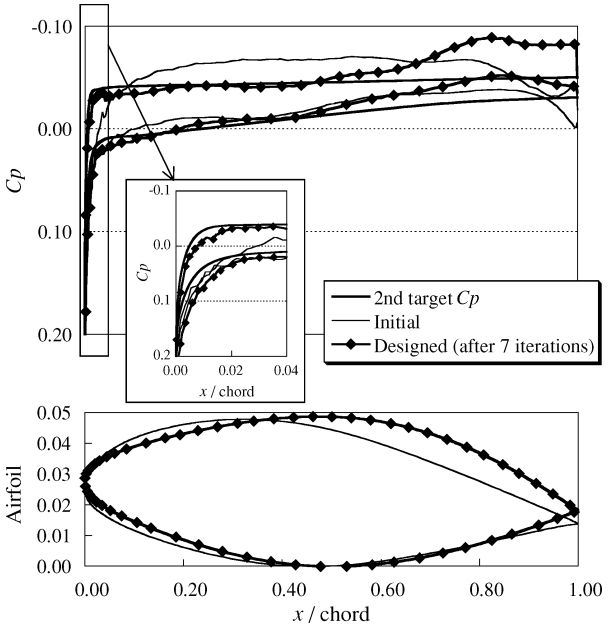

Fig. 17 Initial, final, and target *Cp* distributions and corresponding airfoil profiles at 20% semispan.

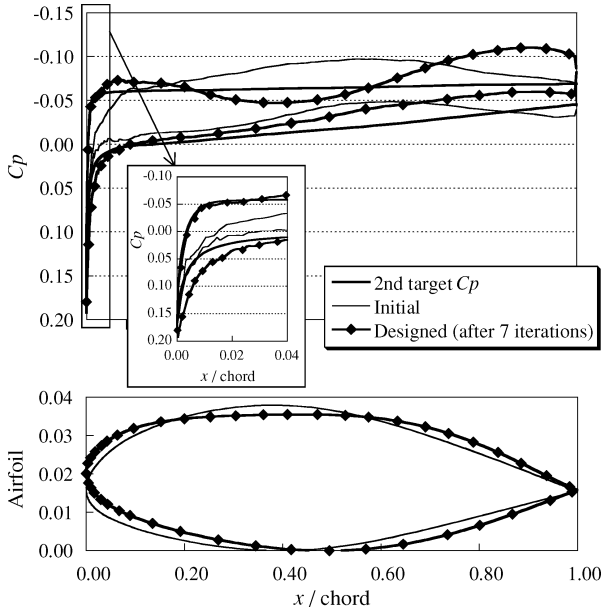

Fig. 18 Initial, final, and target *Cp* distributions and corresponding airfoil profiles at 40% semispan.

is performed before CAD input to check smoothness of the designed geometry. If the geometry is oscillating in the spanwise direction, a further smoothing technique is applied, or a specific airfoil at a certain span station that causes the trouble is disregarded.

Modification of Target *Cp*

An arbitrarily specified pressure distribution does not always correspond to a physically acceptable solution. Therefore, the specified pressure should be modified, as long as the modification would not disturb the concept. With this policy, the validated is made that the Cp^T distribution after second iteration of the design loop is performed. It can be seen that most of the changes to the geometry take place within the first two iterations. In this study, however, the *Cp* did not reach the expansion level of the Cp^T in the vicinity of the leading edge as shown in Fig. 16. We concluded that the first Cp^T was not realistic, and thus the new Cp^T was redefined by adjusting the original one slightly to a higher level of pressure. It was confirmed that the new Cp^T realized the NLF. These two targets are shown in Fig. 16. This change caused a deviation between the Cp^T and the realized Cp^C, and this deviation was smaller than the first one without adjustment.

Designed Geometry

The initial, final, and target *Cp* distributions and the corresponding airfoil shapes are shown in Figs. 17 and 18. As for the airfoil geometry, the thickness constraint is perfectly satisfied. The *Cp* of the upper surface before the 50% chord length at the 20% semispan station agrees well with the Cp^T. The deviation between the Cp^T and the Cp^C at the 40% semispan station, however, is not sufficiently small. It was difficult to realize the Cp^T at the 40% semispan station because of the thickness constraint. However, rapid expansion at the leading edge was realized.

The initial and final pressure distributions over the wing surface are shown in Fig. 19. A region where pressure forms a step-function-type distribution becomes wider at the upper surface of the final model. A flat-roof-type region at the upper surface is expanded near the leading edge, as shown in Fig. 19. At all span stations, a rapid expansion at the leading edge that is the first priority of this design is realized, and the C_L condition is maintained. The seventh inverse designed model was adopted as the NEXST-2 main wing.

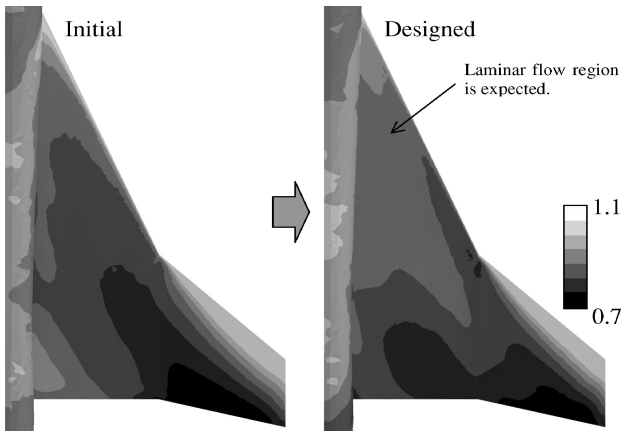

Fig. 19 Comparison of pressure distribution of upper wing at $M_\infty = 1.7$ and $\alpha = 0.6$ deg.

Conclusions

With the aim of realizing a highly practical and efficient aerodynamic design by CFD, an inverse design method coupled with unstructured-mesh CFD was developed. It was applied to the aerodynamic design of wings for the NAL experimental supersonic airplane. The design phase was performed by the inverse problem solver using integral equations. The analysis, phase of the system employed unstructured-mesh CFD closely coupled with the CAD system. Furthermore, interfaces between the design, analysis, and CAD were constructed so as to smoothly transfer the appropriate interface data. Several modification techniques that did not violate the design concept were introduced to satisfy the design constraints and to improve design results. The newly developed method is efficient and has wide applicability to complicated configurations of airplanes. With this method, the wing design of the NEXST-2 model was achieved within a month, a much shorter period than that with the previously employed method.

Acknowledgments

This study was supported by the Industrial Technology Research Grant Program in 2002 from the New Energy and Industrial Technology Development Organization of Japan. The authors would like to thank the aerodynamic group of the NEXST project of National Aerospace Laboratory of Japan for giving us the opportunity to participate in the project. We also would like to thank them for their permission to present geometry data of their Supersonic Transport model in this paper. The calculations were performed using the SGI Origin 2000 and the NEC SX-5 at the Institute of Fluid Science, Tohoku University, and the NEC SX-4 in the Super-Computing System Information Synergy Center, Tohoku University. Also, special thanks go to Y. Ito of the University of Alabama at Birmingham for his help and support with mesh generation.

References

[1]Sakata, K., "Supersonic Experimental Airplane Program in NAL and Its CFD-Design Research Demand," *Proceedings of the 2nd NAL-SST-CFD Workshop*, NAL, Tokyo, Dec. 2000, pp. 53–56.

[2]Shimbo, Y., Yoshida, K., Iwamiya, T., Takaki, R., and Matsushima, K., "Aerodynamic Design of Scaled Supersonic Experimental Airplane," *Proceedings of the 1st NAL-SST-CFD Workshop*, March 1998, pp. 62–67.

[3]Jeong, S., Matsushima, K., Iwamiya, T., Obayashi, S., and Nakahashi, K., "Inverse Design Method for Wings of Supersonic Transport," AIAA Paper 98-0602, Jan. 1998.

[4]Matsushima, K., Iwamiya, T., and Ishikawa, H., "Supersonic Inverse Design of Wings for the Full Configuration of Japanese SST," *Proceedings of the 22nd International Congress of Aeronautical Sciences (ICAS)*, ICAS-2000-2.1.3, UK, Aug.–Sept. 2000, pp. 1–8.

[5]Matsushima, K., "Improper Integrals in the Formulation of a Supersonic Inverse Problem," *Inverse Problems in Engineering Mechanics II*, Elsevier, Oxford, England, UK, 2000, pp. 399–405.

[6]Takanashi, S., "Iterative Three-Dimensional Transonic Wing Design Using Integral Equations," *Journal of Aircraft*, Vol. 22, No. 8, 1985, pp. 654–660.

[7]Dulikravich, G. S., "Shape Inverse Design and Optimization for Three-Dimensional Aerodynamics," AIAA Paper 95-0695, Jan. 1995.

[8]Lomax, H., Heaslet, M. A., and Fuller, F. B., "Integrals and Integral Equations in Linearized Wing Theory," NACA Rept. 1054, NACA Technical Note 2252, 1951.

[9]*Motif CATIA Solutions User's Guide UNIX Workstation Version 4 Release 1*, Dassault Systemes, France, Aug. 1995.

[10]Fujita, T., Ito, Y., Nakahashi, K., and Iwamiya, T., "Computational Fluid Dynamics Evaluation of National Aerospace Laboratory Experimental Supersonic Airplane in Ascent," *Journal of Aircraft*, Vol. 39, No. 2, 2002, pp. 359–364.

[11]Ito, Y., and Nakahashi, K., "Direct Surface Triangulation Using Stereolithography Data," *AIAA Journal*, Vol. 40, No. 3, 2002, pp. 490–496.

[12]Sharov, D., and Nakahashi, K., "A Boundary Recovery Algorithm for Delaunay Tetrahedral Meshing," *Proceedings of the 5th International Conference on Numerical Grid Generation in Computational Field Simulations*, Mississippi State Univ., 1996, pp. 229–238.

[13]Sharov, D., and Nakahashi, K., "Reordering of Hybrid Unstructured Grids for Lower-Upper Symmetric Gause-Seidel Computations," *AIAA Journal*, Vol. 36, No. 3, 1998, pp. 484–486.

[14]Venkatakrishnan, V., "On the Accuracy of Limiters and Convergence to Steady-State Solutions," AIAA paper 93-0880, Jan. 1993.

[15]Obayashi, S., and Guruswamy, G. P., "Convergence Acceleration of a Navier–Stokes Solver for Efficient Static Aeroelastic Computations," *AIAA Journal*, Vol. 33, No. 6, 1995, pp. 1134–1141.

[16]Mavriplis, D. J., and Pirzadeh, S., "Large-Scale Parallel Unstructured Mesh Computations for Three-Dimensional High-Lift Analysis," *Journal of Aircraft*, Vol. 36, No. 6, 1999, pp. 987–998.

[17]Fujita, T., Koizumi, T., Kodera, M., Nakahashi, K., Iwamiya, T., and Nakamura, T., "Evaluation of Parallelized Unstructured-Grid CFD for Aircraft Applications," Parallel Computational Fluid Dynamics, North-Holland, Amsterdam, 2003, pp. 387–394.

[18]Karypis, G., and Kummar, V., "A Fast and High Quality Multilevel Scheme for Partitioning Irregular Graphs," Univ. of Minnesota, Technical Rept. 95-035, 1995.

[19]Jeong, S., Matsushima, K., Iwamiya, T., Obayashi, S., and Nakahashi, K., "Inverse Design of Supersonic Airfoils Using Integral Equations," *Journal of Aircraft*, Vol. 36, No. 3, 1999, pp. 606–608.